NATIONAL ADVISORY COMMITTEE FOR AERONAUTICS

TECHNICAL NOTE

No. 1811

THE LONGITUDINAL STABILITY OF ELASTIC SWEPT WINGS AT SUPERSONIC SPEED

By C. W. Frick and R. S. Chubb

Ames Aeronautical Laboratory
Moffett Field, Calif.

Washington
February 1949

NATIONAL ADVISORY COMMITTEE FOR AERONAUTI(

TECHNICAL NOTE NO. 1811

THE LONGITUDINAL STABILITY OF ELASTIC SWEPT WINGS AT SUPERSONIC SPEED

By C. W. Frick and R. S. Chubb

SUMMARY

The longitudinal stability characteristics of elastic swept wings of high aspect ratio experiencing bending and torsional deformations are calculated for supersonic speed by the application of linearized lifting-surface theory. A parabolic wing deflection curve is assumed and the analysis is simplified by a number of structural approximations. The method is thereby limited in application to wings of high aspect ratio for which the root effects are small. Expressions for the lift, pitching-moment, and span load distribution characteristics are derived in terms of the elastic properties of the wing; namely, the design stress, the modulus of elasticity, the shearing modulus, and the maximum design load factor. The analysis applies to wings with leading edges swept behind the Mach lines. In all cases, however, the trailing edge is sonic or supersonic. Application of the method of analysis to wings with leading edges swept ahead of the Mach lines is discussed.

The results of numerical calculations for a wing of aspect ratio 3.2 and 60° sweepback are presented for a Mach number of 1.414 and for incompressible flow. The effects of wing elasticity on the lift-curve slope, moment-curve slope, and neutral-point position are shown. The results indicate that the primary variable involved in aeroelastic phenomena is the dynamic pressure and that the influence of the flight Mach number is small for wings swept behind the Mach lines.

INTRODUCTION

In reference 1, R. T. Jones has shown that supersonic flight may be attained with a reasonable degree of efficiency through the use of swept wings of high aspect ratio. The use of sweepback, however, involves many problems of stability and control, not the least of which are associated with the aerodynamic effects

of the elastic deformation of the airplane structure. In particular, the longitudinal stability of the aircraft may be affected to a large degree since the bending and torsional deformations of the wing may shift the center of pressure of the lift forward an appreciable distance.

These aeroelastic phenomena occur under those flight conditions where the magnitude and/or the spanwise variation of the elastic deformation of the wing varies with angle of attack. Aeroelastic effects may therefore occur either in accelerated flight at constant dynamic pressure or, under certain conditions, in steady level flight with varying dynamic pressure. In the latter case, if the loading due to twist or camber is different than the loading due to change of angle of attack, the trim change due to elastic deformation of the wing in steady level flight varies with the dynamic pressure and influences the stability of the airplane as indicated by the position of the control stick as a function of airspeed.[1]

In solving aeroelastic problems, since the interrelation of the structural and aerodynamic characteristics of the wing results in mathematical complexity, it is usually necessary to compromise to some extent either the structural or the aerodynamic aspects of the problem to obtain a solution. In the present analysis, the structural characteristics of the wing are compromised to the extent that the form of the deflection curve is assumed. This assumption permits the application of supersonic lifting-surface theory to the determination of the load distribution, the lift, and the pitching-moment characteristics of elastic wings. Additional analysis is necessary to determine whether it is better to use more rigorous aerodynamic theory in aeroelastic computations, as in the present report, or to use a more complete structural theory as in recent work by John W. Miles of U.C.L.A. or Franklin Diederich of the NACA.

SYMBOLS

x_1, y_1 Cartesian coordinates

x, y transformed Cartesian coordinates in terms of the semispan dimension, s

[1]This particular aeroelastic characteristic is not considered in the present report which is concerned primarily with accelerated flight. Further, the wing is considered to be weightless so that the ameliorating influence of the distributed mass of the wing is not accounted for in estimating the aeroelastic characteristics.

ξ,η	x,y coordinates of the apex of any superposed lifting sector
s	distance in the y_1 direction from the root section to the intersection of the flexural axis and the tip Mach cone
s'	distance along the flexural axis from the root section to the intersection of the flexural axis and the tip Mach cone
y'	distance measured from the root section along the flexural axis
$\overline{Y}$	spanwise distance in y direction from the root section to the center of load on the half wing
S	wing area
λ	taper ratio, ratio of tip chord to root chord
c_{av}	average chord
$\overline{c}$	mean aerodynamic chord $\left(\frac{\int c^2 dy}{\int c\ dy}\right)$
c	local chord parallel to the plane of symmetry
c_o	root chord parallel to the plane of symmetry in terms of the span dimension, s
AR	aspect ratio
Λ	angle of sweepback of the flexural axis
θ	slope of the flexural axis in a vertical plane passing through the flexural axis
n	maximum load factor
M	bending moment at any point on the flexural axis
M_r	bending moment at the root section of the wing beam
T	torsional moment at any point on the flexural axis

T_r	torsional moment at the root section of the wing beam
E	modulus of elasticity for the wing beam material
G	shearing modulus for the wing beam material
I	moment of inertia of the wing beam
J	torsional stiffness constant
ζ	distance between the flexural axis and the center of pressure of the sectional lift in terms of the local chord
σ_{max}	maximum design stress
d_r	maximum thickness of the wing at the root section
α	angle of attack of the root section of the wing
α_T	incremental angle of attack at any spanwise station of the wing
α_s	angle of attack of the wing section at any spanwise station
α_n	angle of attack of the root section at which maximum load factor is developed
β	$\sqrt{M^2-1}$ where M is the free-stream Mach number
m	β times the cotangent of the angle of sweepback of the wing leading edge
m_t	β times the cotangent of the angle of sweepback of the wing trailing edge
t	β times the cotangent of the angle of sweepback of a ray from the apex of any superposed lifting sector
Σ	complete elliptic integral of the second kind with modulus $(\sqrt{1-m^2})$
W	airplane weight

$\frac{W}{S}$ wing loading

q dynamic pressure $\left(\frac{1}{2}\rho V^2\right)$, where ρ is the mass density and V the velocity of the free stream

$\frac{\Delta p}{q}$ lifting pressure coefficient

l load per unit span

c_l section lift coefficient

L lift

C_L lift coefficient $\left(\frac{L}{qS}\right)$

C_{L_n} lift coefficient at maximum load factor

m_s section pitching moment of a wing section about the apex of the wing

C_m pitching-moment coefficient about the apex of the wing in terms of the mean aerodynamic chord and the wing area

C_{L_α} the rate of change of lift coefficient with the angle of attack of the root section

C_{m_α} the rate of change of pitching-moment coefficient with the angle of attack of the root section

$C_{m_{C_L}}$ the rate of change of pitching-moment coefficient with the lift coefficient

ANALYSIS

Wing With a Subsonic Leading Edge

In the following analysis, for convenience, the aerodynamic loading due to bending and that due to torsion are first treated separately. Expressions for the combined effects of bending and torsion are derived later.

Bending.- The aerodynamic twist[2] due to bending of a streamwise section of an elastic swept wing under accelerated flight

[2]The change in camber of the airfoil sections due to the distortion of the wing surface is, of course, ignored.

conditions is a function of the applied load and the elastic characteristics of the wing beam. In order to arrive at a solution for the aerodynamic properties of the wing without becoming involved in laborious graphical analysis, some simplifying approximations must be made regarding the elastic properties of the wing.

In a strict sense, a swept wing of conventional structural design cannot be considered to have a flexural axis. For wings of high aspect ratio, however, it will be assumed that a flexural axis exists, since this assumption permits the use of simple beam theory and introduces only a small conservative error.

For the purpose of analysis, the root section of the wing beam is assumed to be the extension of the wing beam on a plane perpendicular to the flexural axis and passing through the intersection of the flexural axis and the streamwise root section. (See fig. 1.) This simplification of the beam analysis is similar to that of reference 2. The length of the wing beam s' is taken as the distance along the flexural axis from the root to the intersection of the flexural axis and the tip Mach cone. The semispan s of the wing is taken as extending from the root section to the intersection of the flexural axis and the tip Mach cone in a direction perpendicular to the plane of symmetry. The portion of the wing lying within the tip Mach cone is ignored since, as shown in reference 3, very little load is carried in this region and the analysis is thereby simplified.

The coordinate system is selected as shown in figure 2. The origin of the coordinate system is placed at the apex of the wing, the positive branch of the x_1 axis lying downstream.

The mathematical treatment may be made less tedious by transforming and nondimensionalizing the coordinates so that in the following analysis

$$y = \frac{\beta y_1}{s}$$

$$x = \frac{x_1}{s}$$

$$c_o = \frac{\text{root chord}}{s}$$

In general, at both subsonic and supersonic speeds, selection of the wing plan form for low drag leads to a combination of spanwise loading and spanwise distribution of the bending resistance in the wing beam such that the wing deflection curve is essentially parabolic. (The ratio of M to I is constant across the span.) The deflection curve

deviates appreciably from a parabola only if the aeroelastic effects experienced by the wing are very large. Calculations show that, for the usual tapered wing, the assumption of a parabolic deflection curve gives results comparable to a more rigorous structural treatment for deviations from rigid wing values as large as, for instance, a 30-percent loss in lift-curve slope. It seems improbable that a designer would be interested in wings with larger deviations from rigid-wing characteristics.

Since the deflection curve of the flexural axis is assumed to be parabolic, the slope of the flexural axis is

$$\theta = \frac{M}{EI} y'$$

where y' is measured along the flexural axis.

The incremental angle of attack of streamwise sections of the wing is related to the slope of the flexural axis as

$$\alpha_T = -\theta \sin \Lambda$$

The slope of the flexural axis in nondimensional transformed coordinates may be written as

$$\theta = \frac{M}{EI} \frac{s}{\beta \cos \Lambda} y$$

The incremental angle of attack of any streamwise section of the elastic wing is then

$$\alpha_T = -\frac{M}{EI} \frac{s}{\beta} y \tan \Lambda$$

and the total angle of attack of any streamwise section is

$$\alpha_s = \alpha - \frac{M}{EI} \frac{s}{\beta} y \tan \Lambda \qquad (1)$$

where α is the angle of attack of the root section of the wing. Equation (1) gives the magnitude and distribution of twist across the span of the wing if the magnitude of M/EI is known.

The distribution of pressure over the elastic wing due to twist may be determined by applying known conical-flow solutions for supersonic flow. In the linearized theory, the principle of superposition of various solutions may be used to satisfy the particular boundary

conditions of the problem. For the elastic wing, the flow field may be considered to consist of the superposition of two distinct flow fields:

1. The flow about a flat rigid wing at an angle of attack equal to the angle of attack of the root section

2. The flow about a twisted wing for which the angle of attack at the root is zero

The solution for the first flow field is given in references 4 and 5; the second flow field can be obtained by determining the solution for a differential twist $d\alpha_s$ at one station and integrating this solution across the span.

The solution for the pressure distribution at any point, corresponding to a differential twist, must meet the following boundary conditions (fig. 3):

1. Outboard of the station of twist, the angle of attack must be constant and equal to the differential twist.

2. Inboard of the station of twist, the angle of attack of the surface must be zero.

3. Between the swept leading edge and the Mach cone, no lifting pressures may exist.

The conical-flow solution corresponding to these boundary conditions is that for a special lifting sector given by Lagerstrom in reference 6 and is expressed in the notation of the present report as

$$\frac{\Delta p}{q} = \frac{8\alpha}{\beta\pi} \frac{m^{s/2}}{m+1} \sqrt{\frac{1+t}{m-t}} \qquad (2)$$

where t defines a ray from the apex of the sector.

Figure 3 shows both a sketch of the boundary conditions to be met by this solution and a plot of the pressure distribution given by equation (2).

The induced pressure resulting from twist due to bending of the elastic wing may be found by integrating across the span of the wing. This integration corresponds to the superposition of an infinite number of the lifting sectors along the span, each sector having an infinitesimal angle of attack $d\alpha_s$.

The pressure due to twist is then given by

$$\left(\frac{\Delta p}{q}\right)_T = -\frac{8}{\beta^2\pi}\frac{m^{3/2}}{(m+1)}\frac{Ms}{EI}\tan\Lambda\int_0^{\eta_o}\sqrt{\frac{1+t}{m-t}}\,d\eta$$

where

$$t = \frac{y-\eta}{x-\xi} = \frac{m(y-\eta)}{mx-\eta}$$

The x and y coordinates of the apex of any superposed sector are ξ,η.

The integration must be carried out from the root section of the wing $\eta=0$ to the value of $\eta=\eta_o$ corresponding to the last superposed sector, the Mach cone of which encompasses the point x,y under consideration. The value of η_o is found by placing t equal to -1 and solving for η.

$$\eta_o = \frac{m}{m+1}(x+y)$$

The integration yields at any point x,y the pressure due to twist

$$\left(\frac{\Delta p}{q}\right)_T = -\frac{16}{3\beta^2\pi}\frac{m^{5/2}}{(m+1)^2}\tan\Lambda\frac{Ms}{EI}(x+y)\sqrt{\frac{x+y}{mx-y}} \qquad (3)$$

To this expression must be added the conjugate term due to the elastic deformation of the opposite wing panel. The conjugate term may be obtained by substituting $-y$ for y. Then

$$\left(\frac{\Delta p}{q}\right)_T = -\frac{16}{3\beta^2\pi}\frac{m^{5/2}}{(m+1)^2}\tan\Lambda\frac{Ms}{EI}\left[(x+y)\sqrt{\frac{x+y}{mx-y}} + (x-y)\sqrt{\frac{x-y}{mx+y}}\right] \qquad (4)$$

It should be noted that the addition of the conjugate terms adds some very small lifting pressure in the region between the wing leading edge and the Mach cone where no lifting pressure may exist. These pressures may be canceled by the superposition of constant lift sectors as noted in reference 7. Since these extraneous pressures, on the average, amount to about 3 percent of the average pressure coefficient over the adjacent wing surface and, since elimination of those pressures

would change the pressures over the surface only about one-half of 1 percent, it seems that in view of the additional complication involved the cancellation of these pressures is unwarranted.

The total lifting pressure for the elastic wing at an angle of attack is then obtained by adding to equation (4) the solution for the flat lifting wing. For the elastic wing, then

$$\frac{\Delta p}{q} = \frac{4m^2\alpha}{\beta\Sigma\sqrt{m^2-\left(\frac{y}{x}\right)^2}} - \frac{16}{3\beta^2\pi}\frac{m^{5/2}}{(m+1)^2}\tan\Lambda\,\frac{Ms}{EI}\left[(x+y)\sqrt{\frac{x+y}{mx-y}}\right.$$

$$\left. + (x-y)\sqrt{\frac{x-y}{mx+y}}\right] \qquad (5)$$

Examination of this equation shows that the relationship between M/EI and α must be established before the pressure distribution can be calculated. Since for wings with parabolic deflection curves the maximum stress occurs at the point of maximum thickness, usually the root, the maximum stress occurring at maximum load factor is

$$\sigma_{max} = \left(\frac{M}{I}\right)_n \frac{d_r}{2}$$

and since the bending moment at any point on the span is a linear function of the angle of attack,

$$\frac{M}{I} = \frac{2\sigma_{max}}{d_r}\frac{\alpha}{\alpha_n}$$

where σ_{max} is the design stress at maximum load factor, d_r is the thickness of the root section and α_n is the angle of attack at maximum load factor; an expression for α_n is derived later.

The equation for the pressure distribution may then be written as

$$\frac{\Delta p}{q} = \frac{4m^2\alpha}{\beta\Sigma\sqrt{m^2-\left(\frac{y}{x}\right)^2}}$$

$$- \frac{32}{3\beta^2\pi}\frac{m^{5/2}}{(m+1)^2}\tan\Lambda\,\frac{\sigma_{max}}{E}\frac{s}{d_r}\frac{\alpha}{\alpha_n}\left[(x+y)\sqrt{\frac{x+y}{mx-y}} + (x-y)\sqrt{\frac{x-y}{mx+y}}\right] \qquad (6)$$

The load per unit span can be obtained from an integration of equation (6) with respect to x along any streamwise station (y=constant),

$$\frac{l}{q} = s \int_{\frac{y}{m}}^{\frac{y+m_t c_o}{m_t}} \left(\frac{\Delta p}{q}\right)_{y=\text{const.}} dx$$

The integration is carried out from the leading edge of the wing, $x = \frac{y}{m}$ to the trailing edge $x = \frac{y+m_t c_o}{m_t}$ and yields

$$\frac{l}{q} = \frac{4m^2 s\alpha}{\beta\Sigma} f_1(y) - \frac{32}{3\beta^2\pi} \frac{m^{5/2}}{(m+1)^2} \tan \Lambda \frac{\sigma_{max}}{E} \frac{s^2}{d_r} \frac{\alpha}{\alpha_n} f_2(y) \qquad (7)$$

The functions $f_1(y)$ and $f_2(y)$ are given in the appendix since they are somewhat unwieldy.

The lift coefficient may be obtained by an integration of equation (7), spanwise from root to tip.

$$\beta C_L = \frac{2s}{S} \int_o^{\beta} \frac{l}{q} dy$$

The integration yields[3]

$$\beta C_L = \frac{2s^2}{S} \left[\frac{4m^2\alpha}{\beta\Sigma} F_1 - \frac{32}{3\beta^2\pi} \frac{m^{5/2}}{(m+1)^2} \tan \Lambda \frac{\sigma_{max}}{E} \frac{s}{d_r} \frac{\alpha}{\alpha_n} F_2 \right] \qquad (8)$$

The constants F_1 and F_2 are given by equations in the appendix.

This equation may be used to determine the angle of attack at maximum load factor α_n which is needed in the foregoing equations:

---

[3]It may be noted that the ratio s^2/S is essentially the same as one-fourth aspect ratio and that the parameter s/d_r is directly related to s'/d_r, a common structural criterion.

$$\alpha_n = \frac{\beta^2\Sigma}{4m^2F_1}\left[\frac{S}{2s^2}C_{L_n} + \frac{32}{3\beta^3\pi}\frac{m^{5/2}}{(m+1)^2}\tan\Lambda\frac{\sigma_{max}}{E}\frac{s}{d_r}F_2\right] \qquad (9)$$

The pitching-moment characteristics of the elastic wing may be determined by an integration of the pressure distribution given by equation (6).

For any spanwise station, the section pitching moment about the apex of the wing is

$$\frac{m_s}{q} = -s^2\int_{\frac{y}{m}}^{\frac{y+m_tc_o}{m_t}}\left(\frac{\Delta p}{q}\right)_{y=\text{const.}} x\,dx$$

This integration yields

$$\frac{m_s}{q} = -s^2\left[\frac{4m^2\alpha}{\beta\Sigma}f_3(y) - \frac{32}{3\beta^2\pi}\frac{m^{5/2}}{(m+1)^2}\tan\Lambda\frac{\sigma_{max}}{E}\frac{s}{d_r}\frac{\alpha}{\alpha_n}f_4(y)\right] \qquad (10)$$

The functions $f_3(y)$ and $f_4(y)$ are given in the appendix.

The total pitching-moment coefficient about the apex of the wing in terms of the mean aerodynamic chord is found by integration across the span,

$$\beta C_m = \frac{2s}{S\bar{c}}\int_o^\beta \frac{m_s}{q}\,dy$$

$$\beta C_m = -\frac{2}{S}\frac{s^3}{\bar{c}}\left[\frac{4m^2\alpha}{\beta\Sigma}F_3 - \frac{32}{3\beta^2\pi}\frac{m^{5/2}}{(m+1)^2}\tan\Lambda\frac{\sigma_{max}}{E}\frac{s}{d_r}\frac{\alpha}{\alpha_n}F_4\right] \qquad (11)$$

or

$$\beta C_{m_\alpha} = -\frac{2}{S}\frac{s^3}{\bar{c}}\left[\frac{4m^2F_3}{\beta\Sigma} - \frac{32}{3\beta^2\pi}\frac{m^{5/2}}{(m+1)^2}\tan\Lambda\frac{\sigma_{max}}{E}\frac{s}{d_r}\frac{F_4}{\alpha_n}\right] \qquad (12)$$

The constants F_3 and F_4 which are functions of the aspect ratio, taper, and sweepback are given in the appendix.

Torsion.- The previous analysis has ignored the effects of wing twist due to torsion. The solutions obtained are, in reality, those for wings of infinite torsional stiffness. In general, since the flexural axis (or torsion center) is behind the center of pressure at

all spanwise stations of the wing, the twist of the wing due to torsion will tend to compensate for the twist due to bending. For wings having large angles of sweepback such as are necessary for efficient supersonic flight, the aerodynamic twist due to torsion has been calculated to be about 15 to 20 percent of the twist due to bending (for thin wings). In such cases, the effect of the torsional deformation on the spanwise loading may be neglected in calculating the torsional moment. Equation (7) may be utilized in the calculation of the torsional moment in this instance. A complex simultaneous solution is thereby avoided.

An expression for the torsional moment at the root section of the wing beam(perpendicular to the elastic axis) may be obtained by assuming that the distance from the center of pressure to the flexural axis for any section of the wing is a constant percentage of the local chord.

Then

$$\beta \frac{T_r}{q} = s \zeta (\cos \Lambda) \int_0^\beta \frac{l}{q} c \, dy$$

where c is the local streamwise chord given by the equation

$$c = s c_o \left[1 - (1-\lambda) \frac{y}{\beta}\right]$$

Where λ denotes the taper ratio of the wing and ζ the distance from center of pressure of flexural axis in terms of the streamwise chord. The function describing the spanwise loading l/q is given by equation (7).

The equation for the torsional moment at the root may be written as

$$\beta \frac{T_r}{q} = s^2 \zeta c_o \cos \Lambda \int_0^\beta \frac{l}{q} \left[1 - (1-\lambda) \frac{y}{\beta}\right] dy$$

$$\beta \frac{T_r}{q} = s^2 \zeta c_o \cos \Lambda \left[\int_0^\beta \frac{l}{q} dy - \frac{1}{\beta} (1-\lambda) \int_0^\beta \frac{l}{q} y \, dy\right]$$

As will be shown later, it is convenient to derive the ratio of the torsional moment at the root to the bending moment at the root. The bending moment at the root is given as

$$\beta \frac{M_r}{q} = \frac{s^2}{\beta \cos \Lambda} \int_0^{\beta} \frac{l}{q} y \, dy$$

and

$$\frac{T_r}{M_r} = \zeta \, c_0 \cos^2 \Lambda \left[\frac{\beta}{\bar{Y}} - (1-\lambda) \right] \tag{13}$$

where

$$\bar{Y} = \frac{\int_0^{\beta} \frac{l}{q} y \, dy}{\int_0^{\beta} \frac{l}{q} \, dy}$$

and corresponds to the spanwise center of pressure for the load on the half wing. The value of $\bar{Y}$ may be determined by a mechanical or analytical integration of equation (7).

When the assumption is made that the twist due to torsion varies linearly across the span (or that the ratio T/GJ is constant across the span), the incremental angle of attack of any section of the wing due to torsional deflection may be written as

$$\alpha_T = \frac{\cos \Lambda}{\beta} \frac{Ts'}{GJ} y = \frac{Ts}{GJ} \frac{y}{\beta}$$

or

$$\alpha_T = \frac{Ms}{EI} \frac{y}{\beta} \left(\frac{T_r I_r E}{M_r J_r G} \right)$$

and by adding this expression to the angle of twist due to bending (equation (1)) the total angle of twist of any section is

$$\alpha_s = \alpha - \frac{Ms}{EI} \frac{y}{\beta} \left[\tan \Lambda - \left(\frac{I_r E}{J_r G} \right) \frac{T_r}{M_r} \right] \tag{14a}$$

or

$$\alpha_s = \alpha - 2 \frac{s}{d_r} \frac{\sigma_{max}}{E} \frac{\alpha}{\alpha_n} \frac{y}{\beta} \left[\tan \Lambda - \left(\frac{I_r E}{J_r G} \right) \frac{T_r}{M_r} \right] \tag{14b}$$

Combined bending and torsion.— Expressions for the aerodynamic properties of swept wings experiencing both bending and torsional deformation may be obtained from equations (6) to (12) if $\tan \Lambda$ is replaced by

$$\left[\tan \Lambda - \left(\frac{I_r E}{J_r G} \right) \frac{T_r}{M_r} \right]$$

The equation for the angle of attack at maximum load factor for combined bending and torsion is then

$$\alpha_n = \frac{\beta^2 \Sigma}{4m^2 F_1}\left\{\frac{8}{2s^2} C_{L_n} + \frac{32}{3\beta^3\pi}\frac{m^{5/2}}{(m+1)^2}\frac{\sigma_{max}}{E}\frac{s}{d_r}\left[\tan\Lambda - \left(\frac{I_r E}{J_r G}\right)\frac{T_r}{M_r}\right]F_2\right\} \quad (15)$$

where

$$\frac{T_r}{M_r} = \zeta\, c_o \left[\frac{\beta}{\bar{Y}} - (1-\lambda)\right] \cos^2\Lambda$$

In applying the foregoing analysis to a specific wing, it is convenient to use the equations to obtain the ratio of C_{m_α} or C_{L_α} for the elastic wing to the value for the rigid wing. Multiplying this ratio by the value of C_{L_α} or C_{m_α} for the rigid wing as determined by the complete theory wherein the region within the Mach cone of the tip, and so forth, is considered, will then give more accurate parameters for the elastic wing. Then

$$\frac{l}{q\alpha} = \frac{4m^2 s}{\beta\Sigma} f_1(y) - \frac{32}{3\beta^2\pi}\frac{m^{5/2}}{(m+1)^2}\frac{\sigma_{max}}{E}\frac{s^2}{d_r}\frac{f_2(y)}{\alpha_n}\left[\tan\Lambda - \left(\frac{I_r E}{J_r G}\right)\frac{T_r}{M_r}\right] \quad (16)$$

$$\frac{C_{L_\alpha}{}_{elastic}}{C_{L_\alpha}{}_{rigid}} = 1 - \frac{8}{3}\frac{\Sigma\sqrt{m}}{\beta\pi(m+1)^2}\frac{\sigma_{max}}{E}\frac{s}{d_r\alpha_n}\left[\tan\Lambda - \left(\frac{I_r E}{J_r G}\right)\frac{T_r}{M_r}\right]\frac{F_2}{F_1} \quad (17)$$

$$\frac{C_{m_\alpha}{}_{elastic}}{C_{m_\alpha}{}_{rigid}} = 1 - \frac{8}{3}\frac{\Sigma\sqrt{m}}{\beta\pi(m+1)^2}\frac{\sigma_{max}}{E}\frac{s}{d_r\alpha_n}\left[\tan\Lambda - \left(\frac{I_r E}{J_r G}\right)\frac{T_r}{M_r}\right]\frac{F_4}{F_3} \quad (18)$$

In using the preceding equations, it is necessary to solve for α_n. This, in turn, involves finding the ratio T_r/M_r which is determined by the parameter $\bar{Y}$ (usually has a value of about 0.40).

A solution of the combined bending and torsional deformation effects can be obtained by assuming a value of $\bar{Y}$, solving for α_n, and checking the value of $\bar{Y}$ from a moment and area integration of a plot of equation (16) to see if a second approximation is required to determine α_n more accurately.

The previous equations apply primarily to flat lifting wings or to twisted and cambered wings for which the loading due to twist and camber is the same essentially as the loading due to change in angle of attack. For wings with somewhat arbitrary camber and/or twist, these equations apply to all accelerated flight conditions. A solution for the aeroelastic characteristics in steady level flight for such wings must involve a consideration of the effects of the loading due to the known arbitrary twist.

Wing With Supersonic Leading Edge

The foregoing analysis has treated wings with the leading edge swept behind the Mach cone. The same method, however, may be applied to wings swept ahead of the Mach cone. In this case, however, the expression for the pressure field for the incremental twist at any spanwise station, corresponding to equation (2), is given by reference 8 as the real part of

$$\frac{\Delta p}{q} = \frac{4\alpha}{\beta\pi}\frac{m}{\sqrt{m^2-1}}\cos^{-1}\frac{1-mt}{|t-m|} \qquad (19)$$

where α, t, and m are as defined for equation (2).

Expressions for the pressure distribution, lift, moment, and load distribution may be obtained in the same manner as for a wing with a subsonic leading edge although the integrations are more involved.

DISCUSSION

Supersonic Lifting-Surface Theory

The results of the foregoing analysis are best illustrated by applying them to a specific wing. For this purpose, the wing shown in figure 4 was selected, having the geometric and structural material characteristics given in the table in the figure. The calculations were made for various values of the parameter $n\frac{W}{S}$ and for two values of the maximum design stress.[4]

Span load distributions for the wing are shown in figure 5 for a Mach number of 1.414, a value of $n\frac{W}{S}$ of 150 pounds per square foot,

[4] Calculations show that the wing has sufficient depth to withstand the maximum loading assumed without failure.

a design stress of 30,000 pounds per square inch, and a dynamic pressure of 211 pounds per square foot which corresponds to flight at 60,000 feet altitude. The load distribution curves of part (a) of figure 5 are for the same angle of attack of the root section and show that the elasticity of the wing results in an appreciable decrease in lift-curve slope. In this case, the reduction experienced by the elastic wing amounts to 15 percent of the value for the rigid wing of the same plan form. Part (b) of figure 5 shows the load distribution curves for constant total lift coefficient. These load distributions are of significance in illustrating how the change in span load distribution due to elasticity may be expected to shift the longitudinal center of pressure forward. The load distributions as derived by what is known as strip theory are discussed later.

Comparison of Aeroelastic Effects at Supersonic Speed With Incompressible Flow Solutions

In calculating lift and stability characteristics of elastic wings, it should be noted that errors resulting from assuming the extent of the wing beam as given in figure 1 and from ignoring the lift within the tip Mach cone may be minimized by using the analytical expressions which give the ratio of lift-curve slope or the ratio of moment-curve slope for the elastic wing to that for the rigid wing. These ratios may be used with the rigorous values of C_{m_α} and C_{L_α} from reference 3 to obtain accurate values of C_{m_α} and C_{L_α} for the elastic wing.

Such ratios have been computed for the wing shown in figure 4 as functions of the dynamic pressure at a flight Mach number of 1.414. For comparison, the same ratios have been computed as functions of the dynamic pressure for incompressible flow by the theory of reference 9. Figures 6 and 7 show the results of these calculations which were made for two values of $n\frac{W}{S}$ of 150 and 300 pounds per square foot and two values of design stress, 30,000 and 45,000 pounds per square inch. Figure 8 shows the shift in neutral point[5] due to wing elasticity as calculated from the data of figures 6 and 7.

The results indicate that the aeroelastic phenomena are a little more severe at supersonic speed, although the aeroelastic effects are found to be primarily a function of the dynamic pressure and not of Mach number. At a given dynamic pressure the differences in the aeroelastic effects as computed by incompressible flow theory and by

[5]Neutral point is defined as the position of the center of gravity along the mean aerodynamic chord for neutral stability.

supersonic lifting-surface theory are found to be due largely to the fact that the center of pressure of the sectional lift is farther forward at subsonic speed, resulting in a difference in torsional deformation which compensates somewhat for the bending deformation. The comparison indicates that the dynamic pressure is the primary variable involved in determining the aeroelastic characteristics, at least for wings swept behind the Mach lines.

It should be noted that the variation of the aeroelastic characteristics with dynamic pressure given in figures 6, 7, and 8 for any value of $n\frac{W}{S}$ and σ_{max} includes the effect of a small variation in wing beam moment of inertia which comes about from the manner in which the maximum design stress was brought into the analysis. The effect is not significant within the range of dynamic pressure for which the theory applies.

In regard to the range of application of the equations, calculations made using more rigorous structural theory with simple strip theory show that the method of the present report may be expected to give accurate estimates of aeroelastic effects as great as, for instance, a 30-percent loss in lift-curve slope. Within such limits it is expected that the estimate of the neutral point shift due to elasticity will be much more accurate than for analyses using elementary aerodynamic loading.

Strip Theory

The analytical evaluation of aeroelastic effects can be greatly simplified by the use of strip theory. This simplified method of determining the aerodynamic loading is based on the assumption that the loading at any spanwise station of the wing is a function only of the section angle of attack. For the present case, a modified strip theory suggests itself wherein only the incremental lift change due to elasticity is considered to be a function of the incremental local angle-of-attack change due to elasticity. The loading at any spanwise station is then given by the product of the ratio of the local angle of attack to the angle of attack of the root section and the expression for the rigid wing loading at any spanwise station. Then, for strip theory

$$\frac{l}{q\alpha} = \frac{4m^2 s}{\beta\Sigma} f_1(y) \frac{\alpha_s}{\alpha}$$

The load distributions so calculated are compared with supersonic lifting-surface theory on figure 5. It is evident that this form

of strip theory overestimates the effects of wing elasticity, but the comparison indicates that the accuracy of strip theory in predicting lift-curve slope is satisfactory. The shift in center of pressure which strip theory gives, however, is much too conservative.

It is suggested, however, that the modified form of strip theory may prove very useful in estimating the effects of wing elasticity on certain aerodynamic parameters, the damping in roll for instance. Further, the use of modified strip theory permits the structural characteristics of the airplane wing to be brought into the problem more completely and enables the designers to estimate wing characteristics for all modes of deflection.

Ames Aeronautical Laboratory,
National Advisory Committee for Aeronautics,
Moffett Field, Calif.

APPENDIX

MATHEMATICAL DERIVATION OF LOADING FUNCTIONS AND PLAN-FORM CONSTANTS

The functions $f_1(y)$, $f_2(y)$, $f_3(y)$, and $f_4(y)$ and the constants F_1, F_2, F_3, F_4 which appear in equations (7) to (18) of the text are given in this appendix.

The functions $f_1(y)$ and $f_2(y)$ were developed from the following integral:

$$\frac{l}{q} = s \int_{\frac{y}{m}}^{\frac{y+m_t c_o}{m_t}} \left(\frac{\Delta p}{q}\right)_{y=\text{const.}} dx$$

from which

$$f_1(y) = \int_{\frac{y}{m}}^{\frac{y+m_t c_o}{m_t}} \frac{dx}{\sqrt{m^2 - \left(\frac{y}{x}\right)^2}}$$

which yields

$$f_1(y) = \frac{1}{m^2}\sqrt{\left(\frac{m^2}{m_t^2} - 1\right) y^2 + \frac{2m^2}{m_t} c_o y + m^2 c_o^2}$$

and

$$f_2(y) = \int_{\frac{y}{m}}^{\frac{y+m_t c_o}{m_t}} (x+y)\sqrt{\frac{x+y}{mx-y}}\,dx + \int_{\frac{y}{m}}^{\frac{y+m_t c_o}{m_t}} (x-y)\sqrt{\frac{x-y}{mx+y}}\,dx$$

which yields

$$f_2(y) = \left[\frac{2m(y+m_t c_o)+m_t y(5m+3)}{4m^2 m_t^2}\right]\left[\sqrt{(y+m_t c_o+m_t y)\,(my+mm_t c_o-m_t y)}\right]$$

$$+ \left[\frac{3y^2(m+1)^2}{8m^{5/2}}\right]\left[\cosh^{-1}\frac{2m(y+m_t c_o)+m_t y(m-1)}{m_t(m+1)y}\right]$$

$$+ \left[\frac{2m(y+m_t c_o)-m_t y(5m+3)}{4m^2 m_t^2}\right]\left[\sqrt{(y+m_t c_o-m_t y)\,(my+mm_t c_o+m_t y)}\right]$$

$$+ \left[\frac{3y^2(m+1)^2}{8m^{5/2}}\right]\left[\cosh^{-1}\frac{2m(y+m_t c_o)-m_t y(m-1)}{m_t(m+1)y}\right]$$

$$+ \left[\frac{y^2(5m+1)\sqrt{2(1-m)}}{4m^{5/2}}\right] - \left[\frac{3y^2(m+1)^2}{8m^{5/2}}\right]\left[\cosh^{-1}\frac{3-m}{m+1}\right]$$

The constants F_1 and F_2 are evaluated as follows:

$$F_1 = \int_0^{\beta} f_1(y)\,dy$$

which yields for $m_t \neq 1$

$$F_1 = \frac{a\beta - m^2 f}{2m_t m^2 a}\sqrt{m^2 f^2 + 2\beta m^2 f - a\beta^2} + \frac{m_t m c_o^2}{2a}$$

$$+ \frac{m_t f^2}{2a^{3/2}}\left(\cos^{-1}\frac{m^2 f - a\beta}{m m_t f} - \cos^{-1}\frac{m}{m_t}\right)$$

and for $m_t = 1$

$$F_1 = \frac{\beta(1-m^2) - m^2 c_o}{2m^2(1-m^2)}\sqrt{m^2 c_o^2 + 2\beta m^2 c_o + \beta^2(m^2-1)} + \frac{m c_o^2}{2(1-m^2)}$$

$$+ \frac{c_o^2}{2(1-m^2)^{3/2}}\left[\cos^{-1}\frac{\beta(m^2-1) + m^2 c_o}{m c_o} - \cos^{-1} m\right]$$

where

$$a = m_t^2 - m^2$$

$$f = m_t c_o$$

and

$$F_2 = \int_o^\beta f_2(y)\,dy$$

which yields for $m_t \neq 1$

$$F_2 = \left(\frac{e}{12m^2 m_t^2 b}\right)\left[(mf^2)^{3/2} - (\beta df + mf^2 - \beta^2 b)^{3/2}\right]$$

$$+\left[\frac{f(de+4mb)}{8m^2m_t^2b}\right]\left\{\frac{2\beta b-df}{4b}\sqrt{\beta df+mf^2-\beta^2b}+\frac{m^{1/2}df^2}{4b}\right.$$

$$\left.+\frac{m_t^2(m+1)^2f^2}{8b^{3/2}}\left[\cos^{-1}\frac{df-2\beta b}{m_tf(m+1)}-\cos^{-1}\frac{d}{m_t(m+1)}\right]\right\}$$

$$+\left[\frac{\beta^3(m+1)^2}{8m^{5/2}}\right]\left[\cosh^{-1}\frac{\beta d+2mf}{\beta m_t(m+1)}+\cosh^{-1}\frac{\beta h+2mf}{\beta m_t(m+1)}-\cosh^{-1}\frac{3-m}{m+1}\right]$$

$$+\left[\frac{f(m+1)^2}{8m^2}\right]\left\{\frac{f^2(3d^2+4mb)}{8b^{5/2}}\left[\cos^{-1}\frac{df-2\beta b}{m_tf(m+1)}-\cos^{-1}\frac{d}{m_t(m+1)}\right]\right.$$

$$\left.-\frac{3df+2\beta b}{4b^2}\sqrt{mf^2+\beta df-\beta^2b}+\frac{3m^{1/2}df^2}{4b^2}\right\}+\left[\frac{\beta^3(5m+1)\sqrt{2(1-m)}}{12m^{5/2}}\right]$$

$$+\left(\frac{j}{4m^2m_t^2}\right)\left[\frac{(mf^2+\beta hf-\beta^2g)^{3/2}-(mf^2)^{3/2}}{3g}\right]$$

$$+\left[\frac{f(4mg-hj)}{8m^2m_t^2g}\right]\left\{\frac{2\beta g-hf}{4g}\sqrt{mf^2+\beta hf-\beta^2g}+\frac{m^{1/2}f^2h}{4g}\right.$$

$$\left.+\frac{f^2m_t^2(1+m)^2}{8g^{3/2}}\left[\cos^{-1}\frac{hf-2\beta g}{m_tf(m+1)}-\cos^{-1}\frac{h}{m_t(m+1)}\right]\right\}$$

$$+\left[\frac{f(m+1)^2}{8m^2}\right]\left\{\frac{f^2(3h^2+4mg)}{8g^{5/2}}\left[\cos^{-1}\frac{hf-2\beta g}{m_tf(m+1)}-\cos^{-1}\frac{h}{m_t(m+1)}\right]\right.$$

$$\left.-\frac{2\beta g+3hf}{4g^2}\sqrt{mf^2+\beta hf-\beta^2g}+\frac{3m^{1/2}hf^2}{4g^2}\right\}$$

where

$$b = (m_t-m)(m_t+1)$$

$$d = 2m+mm_t-m_t$$

$$e = 2m+5mm_t+3m_t$$

$$f = m_t c_o$$

$$g = (m+m_t)(m_t-1)$$

$$h = 2m-mm_t+m_t$$

$$j = 3m_t+5mm_t-2m$$

For $m_t = 1$

$$F_2 = \left(\frac{7m+3}{4m^2}\right)\left\{\frac{[mc_o^2+\beta c_o(3m-1)+2\beta^2(m-1)]^{3/2}}{6(m-1)} - \frac{(mc_o^2)^{3/2}}{6(m-1)}\right\}$$

$$+\left[\frac{c_o}{2m} - \frac{c_o(3m-1)(7m+3)}{16m^2(m-1)}\right]\left\{\left[\frac{4\beta(m-1)+c_o(3m-1)}{8(m-1)}\right]\left[\sqrt{mc_o^2+\beta c_o(3m-1)+2\beta^2(m-1)}\right]\right.$$

$$-\left[\frac{c_o(3m-1)}{8(m-1)}\right](\sqrt{mc_o^2}) + \left[\frac{c_o^2(m+1)^2}{16\sqrt{2}(1-m)^{3/2}}\right]\left[\cos^{-1}\frac{4\beta(m-1)+c_o(3m-1)}{c_o(m+1)}\right.$$

$$\left.\left. - \cos^{-1}\frac{3m-1}{m+1}\right]\right\}$$

$$+\left[\frac{\beta^3(m+1)^2}{8m^{5/2}}\right]\left[\cosh^{-1}\frac{\beta(3m-1)+2mc_o}{\beta(m+1)} + \cosh^{-1}\frac{\beta(m+1)+2mc_o}{\beta(m+1)} - \cosh^{-1}\frac{3-m}{m+1}\right]$$

$$+\left[\frac{c_o^2(m+1)^2}{8m}\right]\left\{\left[\frac{4\beta(m-1)-3c_o(3m-1)}{16mc_o(m-1)^2}\right]\left[\sqrt{mc_o^2+\beta c_o(3m-1)+2\beta^2(m-1)}\right]\right.$$

$$\left.+\left[\frac{3c_o(3m-1)}{16m^{1/2}(m-1)^2}\right]\right.$$

$$+\left[\frac{c_o(19m^2-10m+3)}{32\sqrt{2}m(1-m)^{5/2}}\right]\left[\cos^{-1}\frac{4\beta(m-1)+c_o(3m-1)}{c_o(m+1)}-\cos^{-1}\frac{3m-1}{m+1}\right]$$

$$+\left\{\frac{2[8m^2c_o^2-4\beta mc_o(m+1)+3\beta^2(m+1)^2]}{15mc_o^{3/2}(m+1)^3}\right\}\left[\sqrt{mc_o+\beta(m+1)}\right]-\frac{16m^{3/2}c_o}{15(m+1)^3}\Bigg\}$$

$$+\left\{\left[\frac{1}{3m(m+1)}\right]+\left[\frac{2mc_o-3\beta(m+1)}{10m^2c_o(m+1)}\right]\right\}\left\{\left[mc_o^2+\beta c_o(m+1)\right]^{3/2}\right\}$$

$$+\left[\frac{\beta^3(5m+1)\sqrt{2(1-m)}}{12m^{5/2}}\right]-\left[\frac{8(mc_o^2)^{3/2}}{15m(m+1)}\right]$$

The functions $f_3(y)$ and $f_4(y)$ were developed from the integral:

$$\frac{m_s}{q}=-s^2\int_{\frac{y}{m}}^{\frac{y+m_tc_o}{m_t}}\left(\frac{\Delta p}{q}\right)_{y=\text{const.}}xdx$$

from which

$$f_3(y)=\int_{\frac{y}{m}}^{\frac{y+m_tc_o}{m_t}}\frac{xdx}{\sqrt{m^2-(y/x)^2}}$$

Then

$$f_3(y)=\frac{y+m_tc_o}{2m^2m_t^2}\sqrt{m^2(y+m_tc_o)^2-m_t^2y^2}$$

$$+ \frac{y^2}{2m^3} \cosh^{-1} \frac{m(y+m_t c_o)}{m_t y}$$

Also

$$f_4(y) = \int_{\frac{y}{m}}^{\frac{y+m_t c_o}{m_t}} (x+y) \sqrt{\frac{x+y}{mx-y}}\, x\,dx + \int_{\frac{y}{m}}^{\frac{y+m_t c_o}{m_t}} (x-y) \sqrt{\frac{x-y}{mx+y}}\, x\,dx$$

which yields

$$f_4(y) = \left[\sqrt{(y+m_t c_o+m_t y)(my+mm_t c_o-m_t y)} \right] \left[\frac{8(y+m_t c_o)^2}{24m\, m_t^3} \right.$$

$$\left. + \frac{2mm_t y(y+m_t c_o)(7m+5)+m_t^2 y^2(3m^2+22m+15)}{24m^3 m_t^3} \right]$$

$$+ \left[\frac{y^3(m^3-3m^2-9m-5)}{16m^{7/2}} \right] \left[\cosh^{-1} \frac{(2m-mm_t+m_t)y+2mm_t c_o}{m_t(m+1)y} \right.$$

$$\left. - \cosh^{-1} \frac{3-m}{m+1} - \cosh^{-1} \frac{(2m+mm_t-m_t)y+2mm_t c_o}{m_t(m+1)y} \right]$$

$$+ \left[\sqrt{(y+m_t c_o-m_t y)(my+mm_t c_o+m_t y)} \right] \left[\frac{8(y+m_t c_o)^2}{24m\, m_t^3} \right.$$

$$\left. - \frac{2mm_t y(y+m_t c_o)(7m+5)-m_t^2 y^2(3m^2+22m+15)}{24m^3 m_t^3} \right]$$

$$- \left[\frac{y^3(3m^2+8m+13)\sqrt{2(1-m)}}{24m^{7/2}} \right]$$

The constant F_3 is evaluated as:

$$F_3 = \int_0^{\beta} f_3(y)dy$$

which yields for $m_t \neq 1$

$$F_3 = \frac{m^3f^3-(m^2f^2+2\beta m^2f-\beta^2a)^{3/2}}{6m_t^2m^2a} + \frac{\beta^3}{6m^3}\cosh^{-1}\frac{m(\beta+f)}{\beta m_t}$$

$$+ \frac{f(a\beta-3m^2f)\sqrt{m^2f^2+2\beta m^2f-a\beta^2}}{6m^2a^2} + \frac{mf^3}{2a^2}$$

$$+ \frac{f^3(2m_t^2+m^2)}{6a^{5/2}}\left(\cos^{-1}\frac{m^2f-a\beta}{mm_t^2c_o} - \cos^{-1}\frac{mf}{m_t^2c_o}\right)$$

and for $m_t = 1$

$$F_3 = \frac{m^3c_o^3-[m^2c_o^2+2\beta m^2c_o-\beta^2(1-m^2)]^{3/2}}{6m^2(1-m^2)} + \frac{\beta^3}{6m^3}\cosh^{-1}\frac{m(\beta+c_o)}{\beta}$$

$$+ \frac{c_o[\beta(1-m^2)-3m^2c_o]\sqrt{m^2c_o^2+2\beta m^2c_o-\beta^2(1-m^2)}}{6m^2(1-m^2)^2} + \frac{mc_o^3}{2(1-m^2)^2}$$

$$+ \frac{c_o^3(2+m^2)}{5(1-m^2)^{5/2}}\left[\cos^{-1}\frac{m^2c_o-\beta(1-m^2)}{mc_o} - \cos^{-1} m\right]$$

Also F_4 is evaluated as:

$$F_4 = \int_0^{\beta} f_4(y)\,dy$$

which yields for $m_t \neq 1$

$$F_4 = \left[\frac{A}{24m^3m_t^3}\left(\beta + \frac{5df}{6b}\right) + \frac{B}{18m^3m_t^3}\right]\left[\frac{(mf^2+\beta df-\beta^2 b)^{3/2}}{-4b}\right]$$

$$+\left\{\frac{2\beta b-df}{4b}\sqrt{mf^2+\beta df-\beta^2 b} + \frac{m_t^2f^2(m+1)^2}{8b^{3/2}}\left[\cos^{-1}\frac{df-2\beta b}{m_tf(m+1)} - \cos^{-1}\frac{d}{m_t(m+1)}\right]\right.$$

$$\left. + \frac{m^{1/2}df^2}{4b}\right\}\left[\frac{Af^2(5d^2+4mb)+8Bbdf+128m^2b^2f^2}{384m^3m_t^3b^2}\right]$$

$$+\left(\frac{5Adf}{144m^3m_t^3b} + \frac{B}{18m^3m_t^3}\right)\left[\frac{(mf^2)^{3/2}}{4b}\right]$$

$$+\left(\frac{C}{4}\right)\left\{\beta^4\left[\cosh^{-1}\frac{\beta h+2mf}{\beta m_t(m+1)} - \cosh^{-1}\frac{3-m}{m+1} - \cosh^{-1}\frac{\beta d+2mf}{\beta m_t(m+1)}\right]\right.$$

$$+ (m^{1/2}f)\left[\left(\frac{\beta^2}{3b} + \frac{5\beta df}{12b^2} + \frac{5d^2f^2}{8b^3} + \frac{2mf^2}{3b^2}\right)\left(\sqrt{mf^2+\beta df-\beta^2 b}\right)\right.$$

$$\left.\left. -\left(\frac{\beta^2}{3g} + \frac{5\beta hf}{12g^2} + \frac{5f^2h^2}{8g^3} + \frac{2mf^2}{3g^2}\right)\left(\sqrt{mf^2+\beta fh-\beta^2 g}\right)\right.\right.$$

$$\left. - \left[\frac{df^3(12mb-5d^2)}{16b^{7/2}}\right]\left[\cos^{-1}\frac{df-2\beta b}{m_tf(m+1)} - \cos^{-1}\frac{d}{m_t(m+1)}\right]\right.$$

$$+\left[\frac{hf^3(12mg+5h^2)}{16g^{7/2}}\right]\left[\cos^{-1}\frac{hf-2\beta g}{m_t f(m+1)}-\cos^{-1}\frac{h}{m_t(m+1)}\right]$$

$$-(f^3m^{1/2})\left(\frac{5d^2}{8b^3}+\frac{2m}{3b^2}-\frac{5h^2}{8g^3}-\frac{2m}{3g^2}\right)\Bigg\}\Bigg]$$

$$+\left[\frac{Df^2(5h^2+4mg)+8Hfgh+128f^2m^2g^2}{384m^3m_t{}^3g^2}\right]\left\{\left(\frac{2\beta g-fh}{4g}\right)\left(\sqrt{mf^2+\beta fh-\beta^2 g}\right)\right.$$

$$\left.+\left(\frac{f^2hm^{1/2}}{4g}\right)+\left[\frac{m_t{}^2f^2(m+1)^2}{8g^{3/2}}\right]\left[\cos^{-1}\frac{fh-2\beta g}{m_t f(m+1)}-\cos^{-1}\frac{h}{m_t(m+1)}\right]\right\}$$

$$-\left[\left(\frac{D}{24m^3m_t{}^3}\right)\left(\beta+\frac{5fh}{6g}\right)+\left(\frac{H}{18m^3m_t{}^3}\right)\right]\left[\frac{(mf^2+\beta fh-\beta^2g)^{3/2}}{4g}\right]$$

$$-\left[\frac{\beta^4(3m^2+8m+13)\sqrt{2(1-m)}}{96m^{7/2}}\right]+\left[\frac{(mf^2)^{3/2}}{4g}\right]\left[\left(\frac{5Dfh}{144m^3m_t{}^3g}\right)+\left(\frac{H}{18m^3m_t{}^3}\right)\right]$$

where

$$A = 8m^2+14m^2m_t+10mm_t+3m^2m_t{}^2+22mm_t{}^2+15m_t{}^2$$

$$B = 2mm_tc_o(8m+7mm_t+5m_t)$$

$$C = \frac{m^3-3m^2-9m-5}{16m^{7/2}}$$

$$D = 8m^2-14m^2m_t-10mm_t+3m^2m_t{}^2+22mm_t{}^2+15m_t{}^2$$

$$H = 2mm_tc_o(8m-7mm_t-5m_t)$$

and for $m_t = 1$

$$F_4 = \left\{\frac{T}{32m^3}\left[\beta-\frac{5c_o(3m-1)}{12(m-1)}\right]+\frac{V}{24m^3}\right\}\left\{\frac{[mc_o{}^2+\beta c_o(3m-1)+2\beta^2(m-1)]^{3/2}}{6(m-1)}\right\}$$

$$+\left\{\frac{T}{32m^3}\left[\frac{5c_o(3m-1)}{12(m-1)}\right]-\frac{V}{24m^3}\right\}\left[\frac{(mc_o{}^2)^{3/2}}{6(m-1)}\right]+\left\{\frac{T}{24m^3}\left[\frac{c_o{}^2(37m^2-22m+5)}{64(m-1)^2}\right]\right.$$

$$-\frac{V}{24m^3}\left[\frac{c_o(3m-1)}{4(m-1)}\right]+\frac{c_o^2}{3m}\left\{\frac{4\beta(m-1)+c_o(3m-1)}{8(m-1)}\left[\sqrt{mc_o^2+\beta c_o(3m-1)+2\beta^2(m-1)}\right]\right.$$

$$\left.+\frac{c_o^2(m+1)^2}{16\sqrt{2}(1-m)^{3/2}}\left[\cos^{-1}\frac{4\beta(m-1)+c_o(3m-1)}{c_o(m+1)}-\cos^{-1}\frac{3m-1}{m+1}\right]+\frac{m^{1/2}c_o^2(3m-1)}{8(1-m)}\right\}$$

$$+\frac{C}{4}\left\{\beta^4\left[\cosh^{-1}\frac{\beta(m+1)+2mc_o}{\beta(m+1)}-\cosh^{-1}\frac{3-m}{m+1}-\cosh^{-1}\frac{\beta(3m-1)+2mc_o}{\beta(m+1)}\right]\right.$$

$$+(mc_o)\left[\frac{2\beta^3\sqrt{m^2c_o^2+\beta mc_o(m+1)}}{7mc_o(m+1)}\right.$$

$$-\frac{4[8m^2c_o^2-4\beta mc_o(m+1)+3\beta^2(m+1)^2]}{35(1+m)^4}\cdot\sqrt{m^2c_o^2+\beta mc_o(m+1)}$$

$$-\left[\frac{\beta^2}{6m(m-1)}-\frac{5\beta c_o(3m-1)}{48m(m-1)^2}\right.$$

$$\left.+\frac{5c_o^2(3m-1)^2}{64m(m-1)^3}-\frac{c_o^2}{6(m-1)^2}\right]\sqrt{2\beta^2m(m-1)+\beta mc_o(3m-1)+m^2c_o^2}$$

$$+\frac{32m^3c_o^3}{35(m+1)^4}+\frac{c_o^3(63m^3-39m^2+21m-5)}{128\sqrt{2m(1-m)}(m-1)^3}\left[\cos^{-1}\frac{4\beta(m-1)+c_o(3m-1)}{c_o(m+1)}\right.$$

$$\left.\left.\left.-\cos^{-1}\frac{3m-1}{m+1}\right]+\frac{5c_o^3(3m-1)^2}{64(m-1)^3}-\frac{mc_o^3}{6(m-1)^2}\right]\right\}$$

$$-\left[\frac{\beta^4(3m^2+8m+13)\sqrt{2(1-m)}}{96m^{7/2}}\right]+\left\{\frac{2c_o}{9m(m+1)}+\frac{(5-m)[2mc_o-3\beta(m+1)]}{90m^2(m+1)^2}\right.$$

$$+\frac{(5-m)[8m^2c_o^2-12\beta mc_o(m+1)+15\beta^2(m+1)^2]}{420m^3c_o(m+1)^2}\Bigg\}\left\{[mc_o^2+\beta c_o(m+1)]^{3/2}\right\}$$

$$-\left[(mc_o^2)^{3/2}\right]\left[\frac{2c_o}{9m(m+1)}+\frac{c_o(5-m)}{45m(m+1)^2}+\frac{2c_o(5-m)}{105m(m+1)^2}\right]$$

where

$$T = 25m^2+32m+15$$

$$V = 10mc_o(3m+1)$$

REFERENCES

1. Jones, R. T.: Estimated Lift-Drag Ratios at Supersonic Speed. NACA TN No. 1350, 1947.

2. Zender, George, and Libove, Charles: Stress and Distortion Measurements in a 45° Swept Box Beam Subjected to Bending and to Torsion. NACA TN No. 1525, 1948.

3. Cohen, Doris: The Theoretical Lift of Flat Swept-Back Wings at Supersonic Speeds. NACA TN No. 1555, 1948.

4. Stewart, H. J.: The Lift of a Delta Wing at Supersonic Speeds. Quart. App. Math., vol. IV, no. 3, Oct. 1946, pp. 246-254.

5. Brown, Clinton E.: Theoretical Lift and Drag of Thin Triangular Wings at Supersonic Speeds. NACA TN No. 1183, 1946.

6. Lagerstrom, P. A.: Linearized Supersonic Theory of Conical Wings. NACA TN No. 1685, 1948.

7. Frick, Charles W., Jr.: Application of the Linearized Theory of Supersonic Flow to the Estimation of Control-Surface Characteristics. NACA TN No. 1554, 1948.

8. Jones, R. T.: Thin Oblique Airfoils at Supersonic Speed. NACA TN No. 1107, 1946.

9. Stevens, Victor I.: Theoretical Basic Span Loading Characteristics of Wings with Arbitrary Sweep, Aspect Ratio, and Taper Ratio. NACA TN No. 1772, 1948.

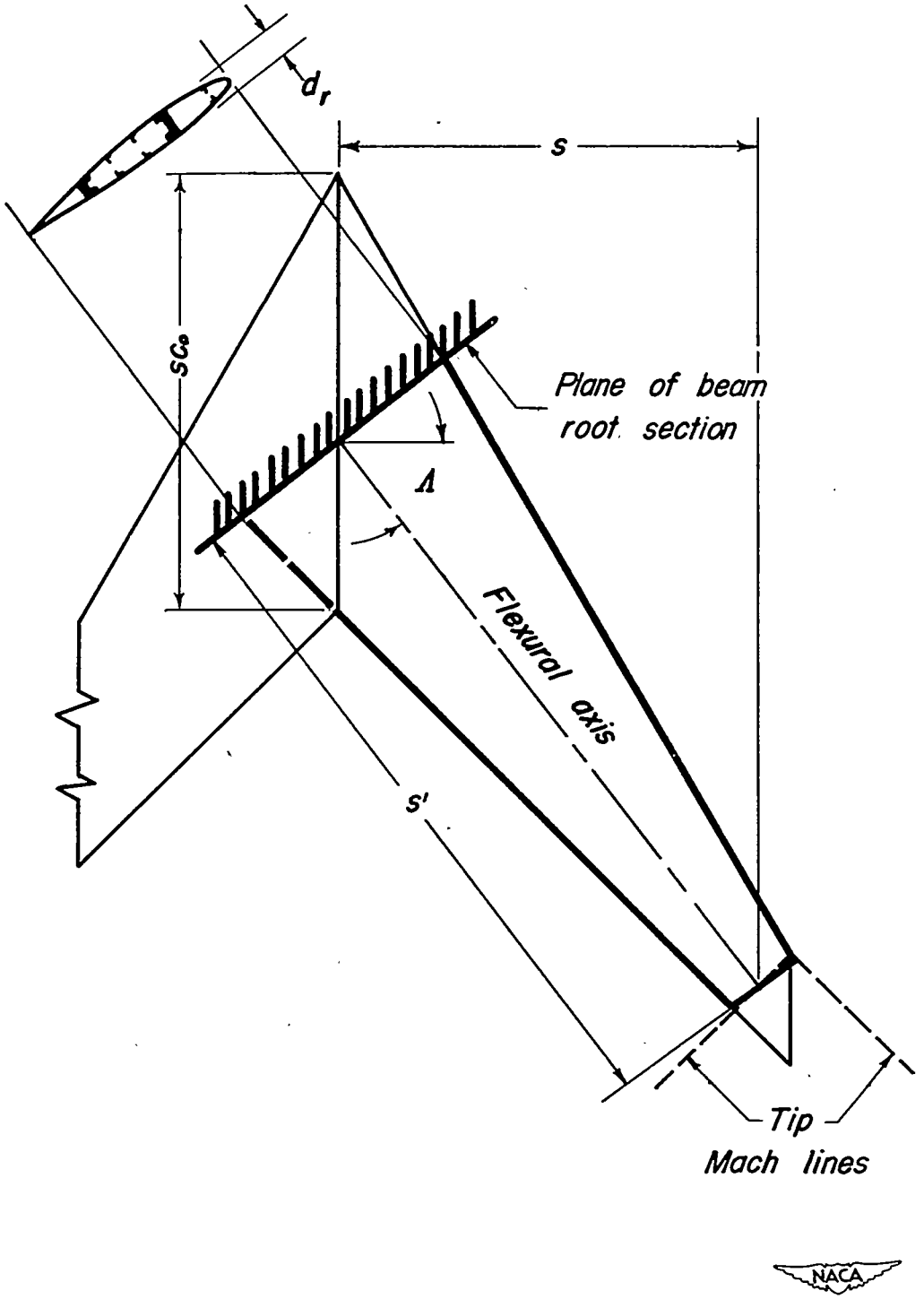

Figure 1. — Geometric characteristics of the wing beam.

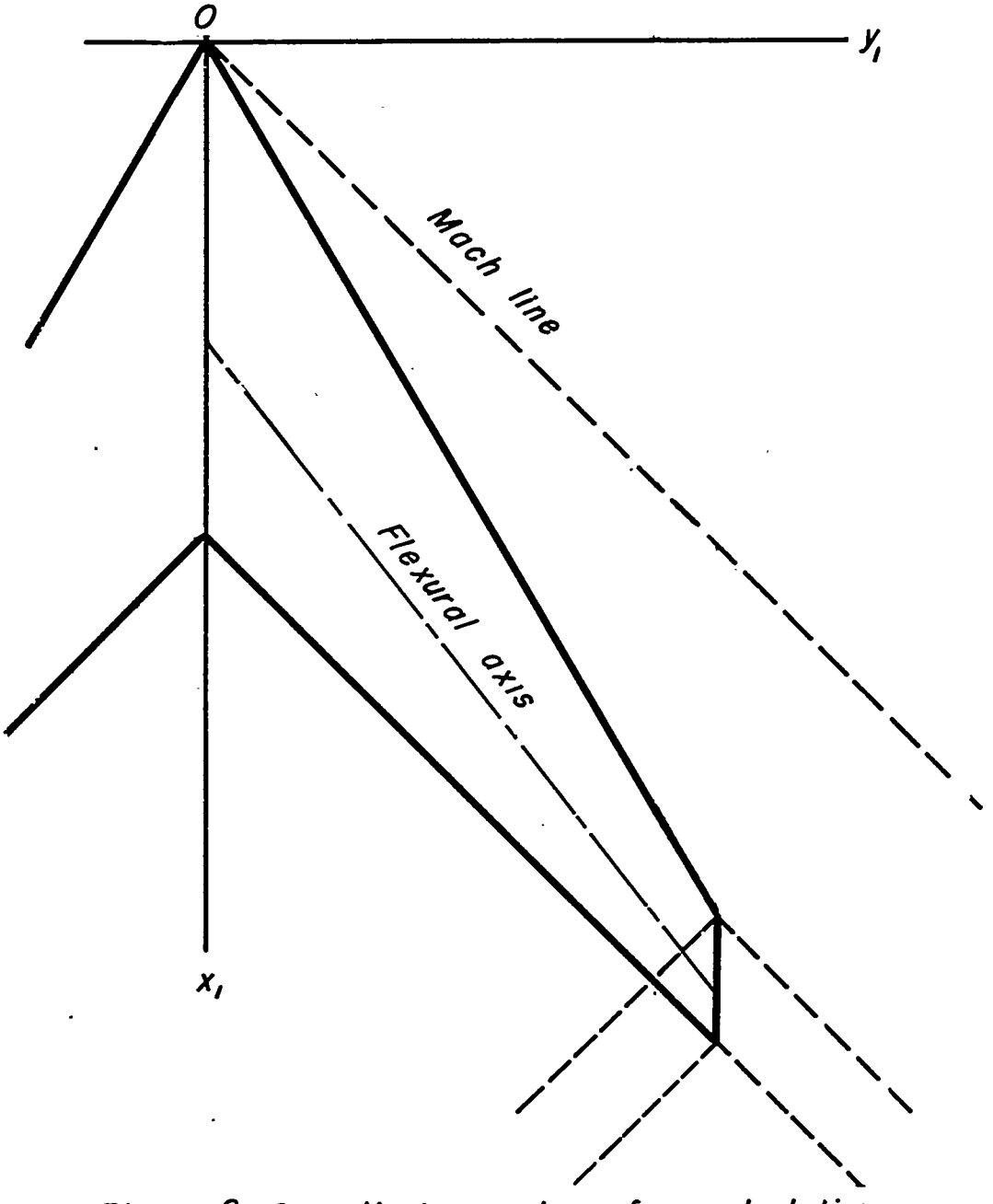

Figure 2.–Coordinate system for calculation of characteristics of elastic wings.

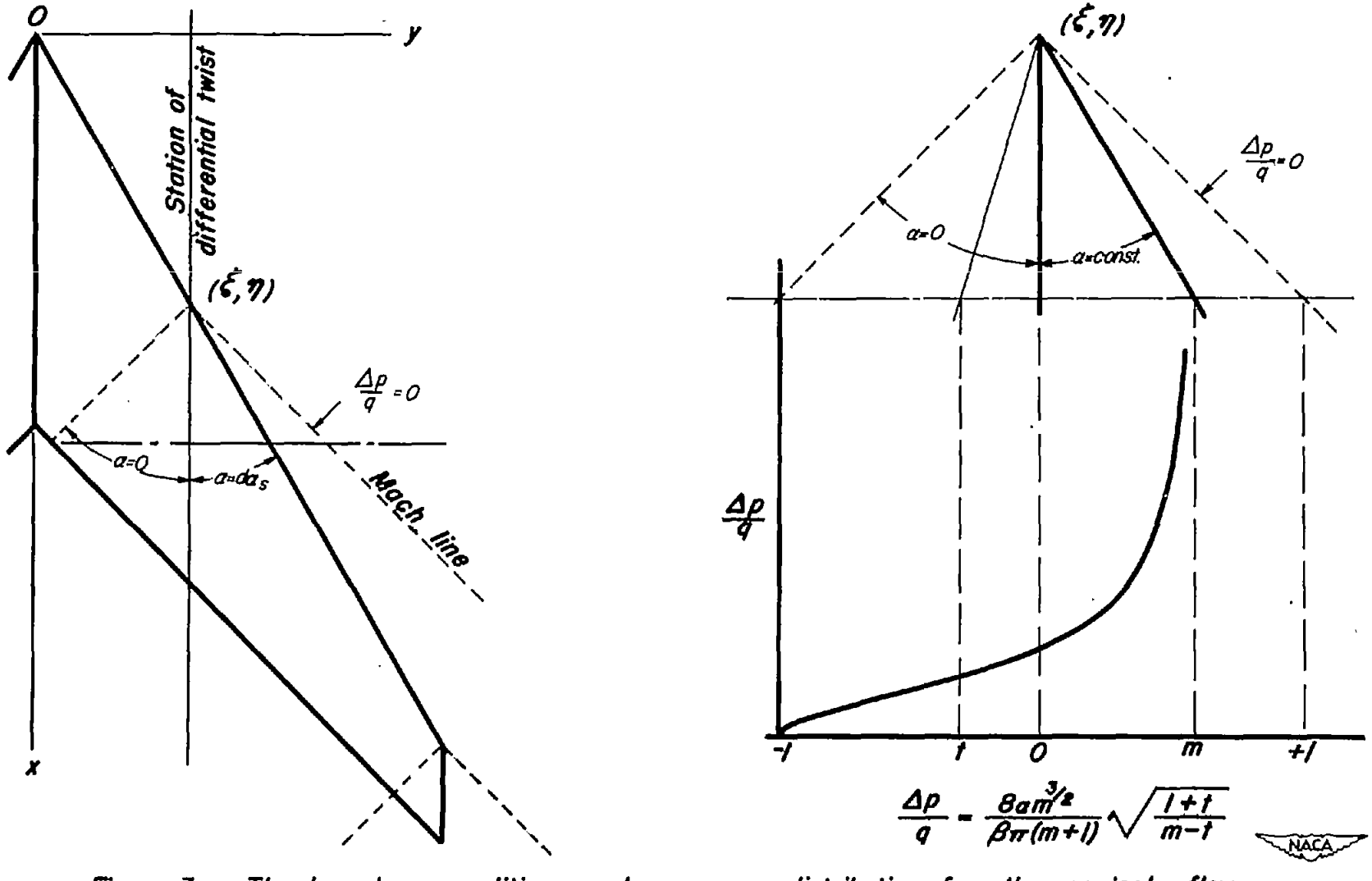

Figure 3.— The boundary conditions and pressure distribution for the conical flow solution for differential twist.

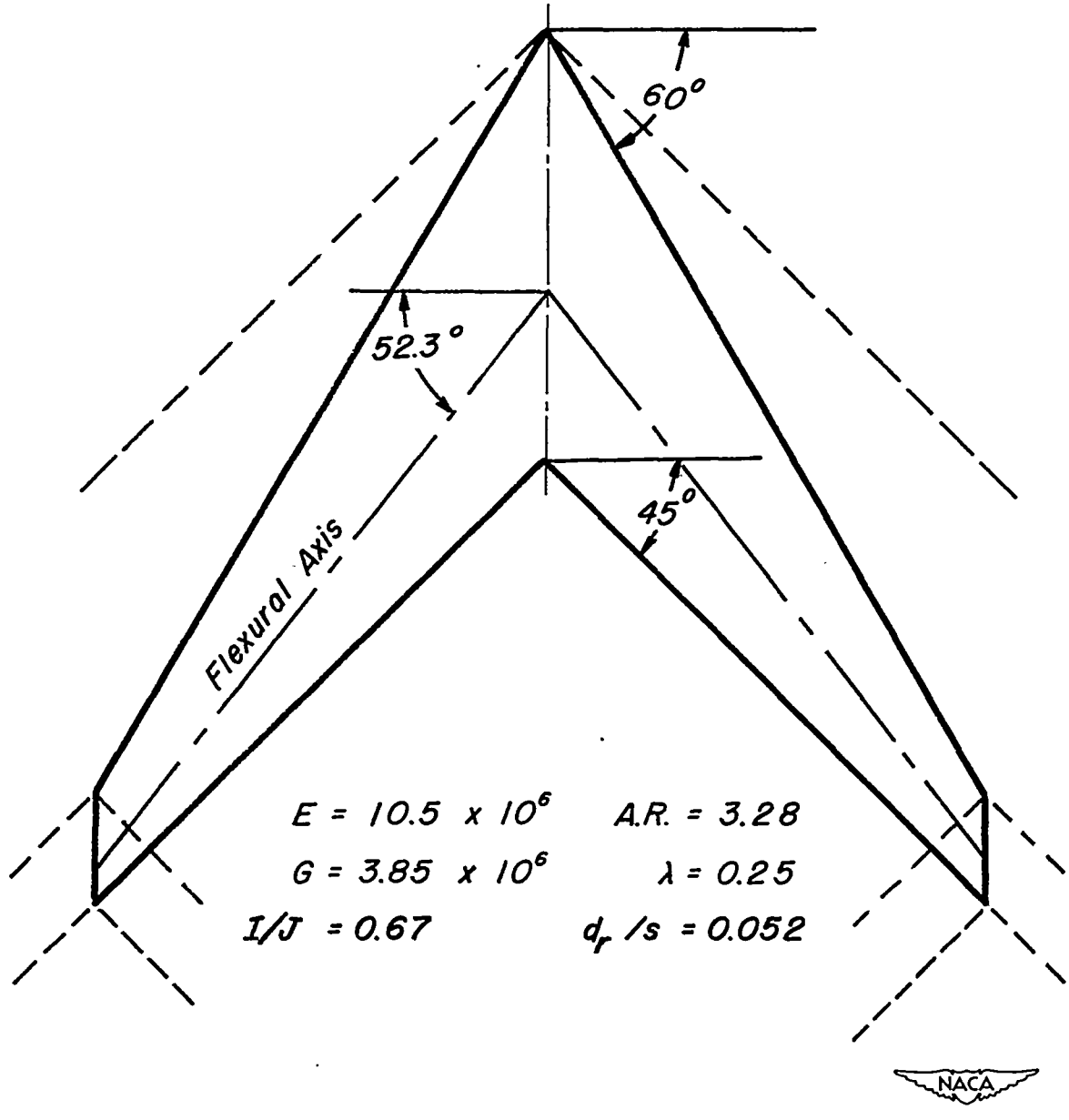

Figure 4.— Sketch of the wing used in the calculations.

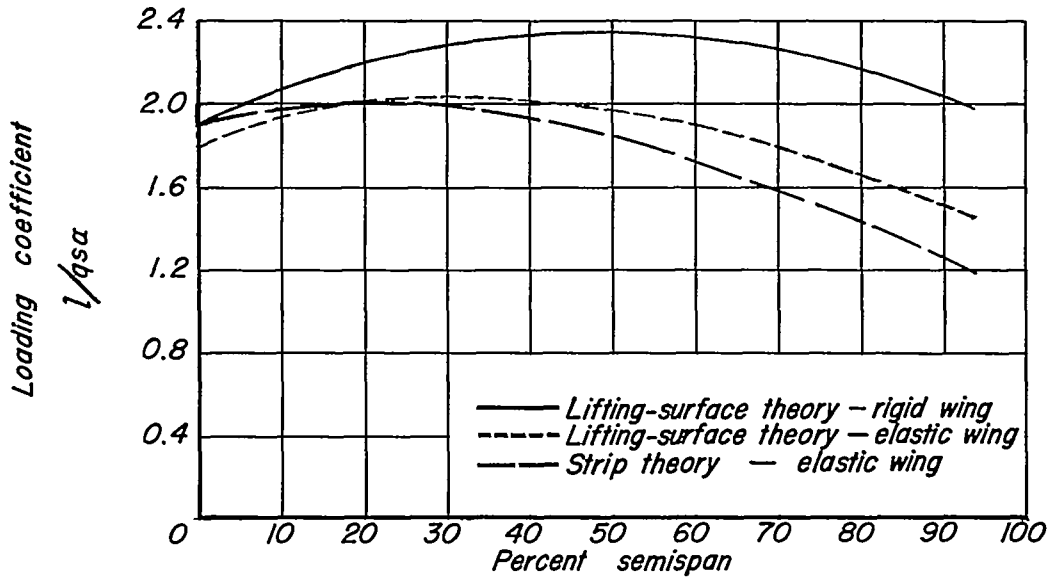

(a) Span load distributions for the rigid and elastic wings at the same angle of attack.

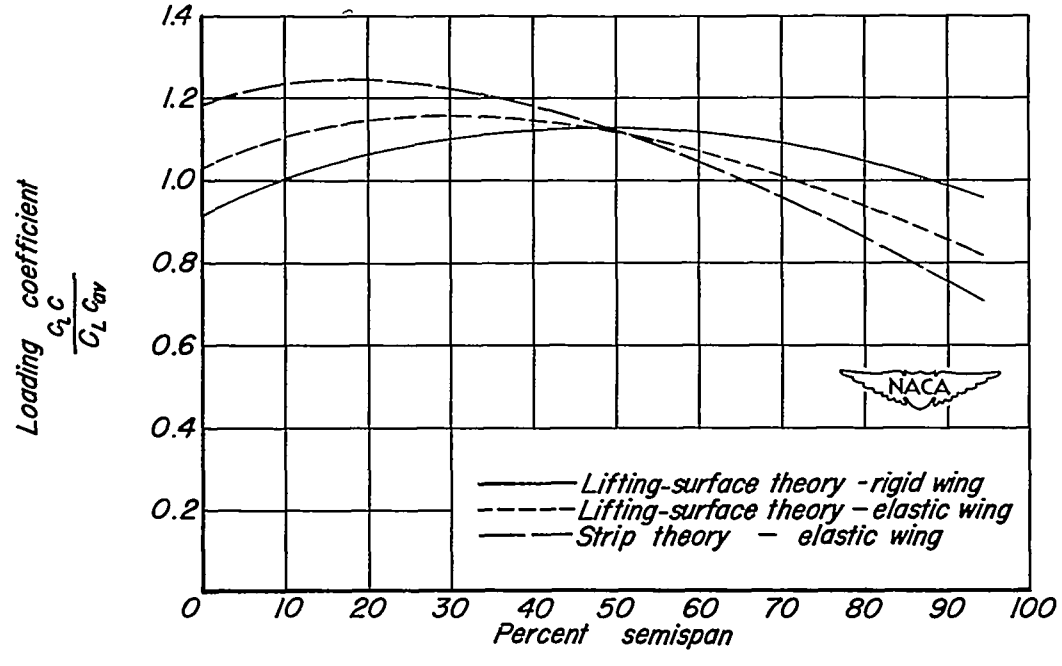

(b) Span load distributions for the rigid and elastic wings at the same total lift coefficient.

Figure 5.— A comparison of the span load distributions for the rigid and the elastic wings in accelerated flight. M, 1.414; σ_{max}, 30,000 pounds per square inch; nW/S, 150 pounds per square foot; q, 211.2 pounds per square foot.

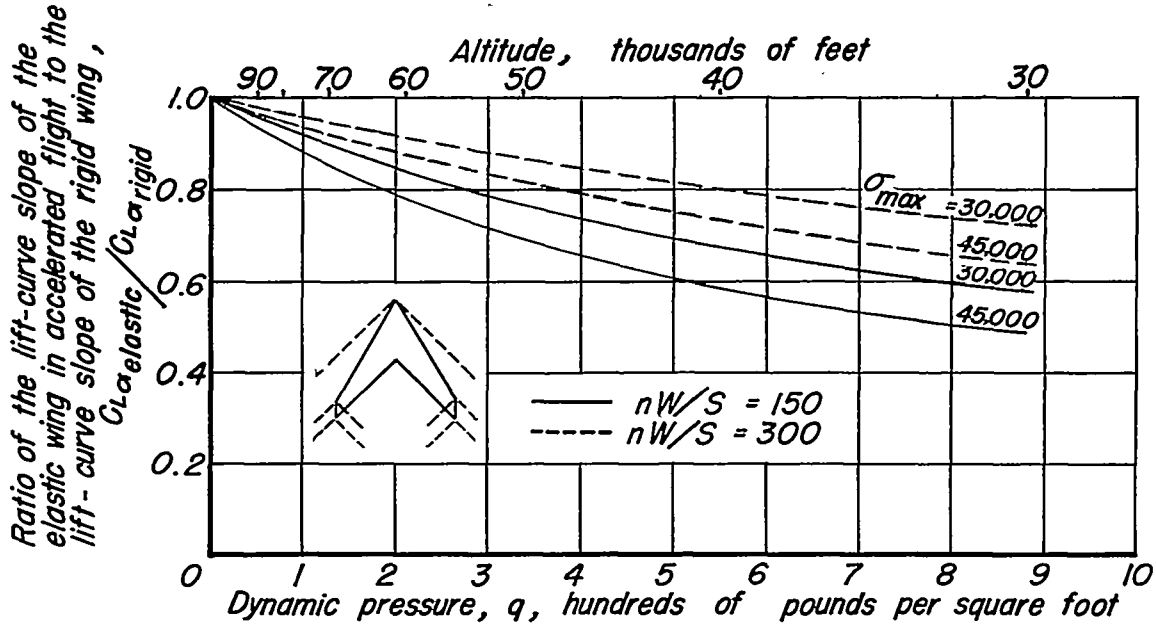

(a) Mach number, 1.414.

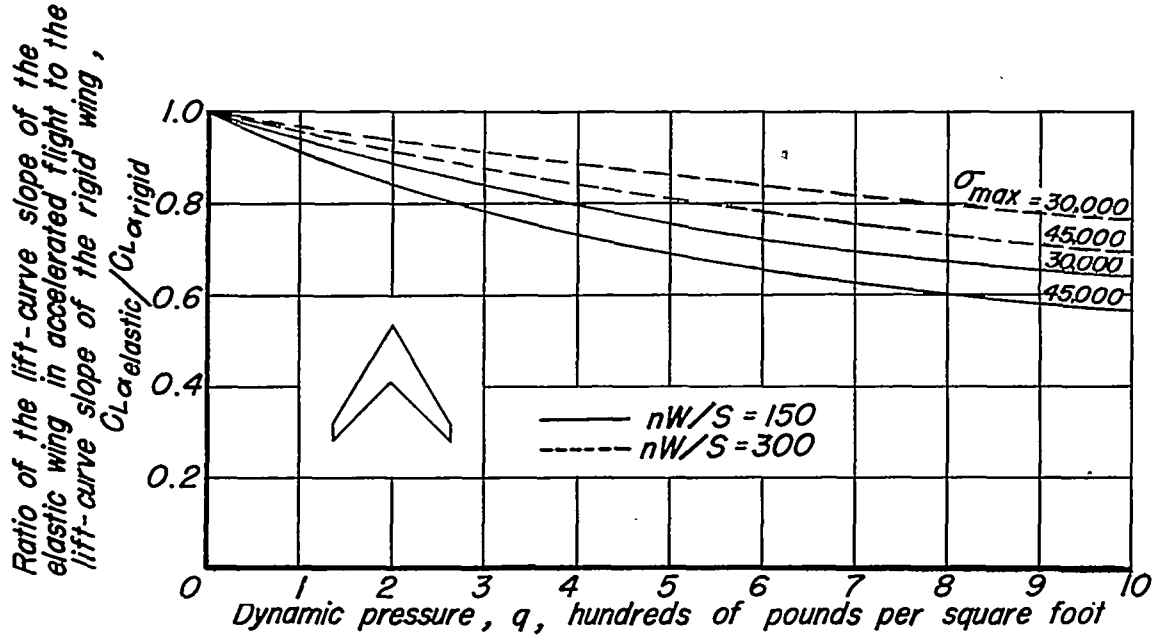

(b) Incompressible flow.

NACA

Figure 6.—Variation with dynamic pressure of the ratio of lift-curve slopes for the elastic and rigid wings in accelerated flight.

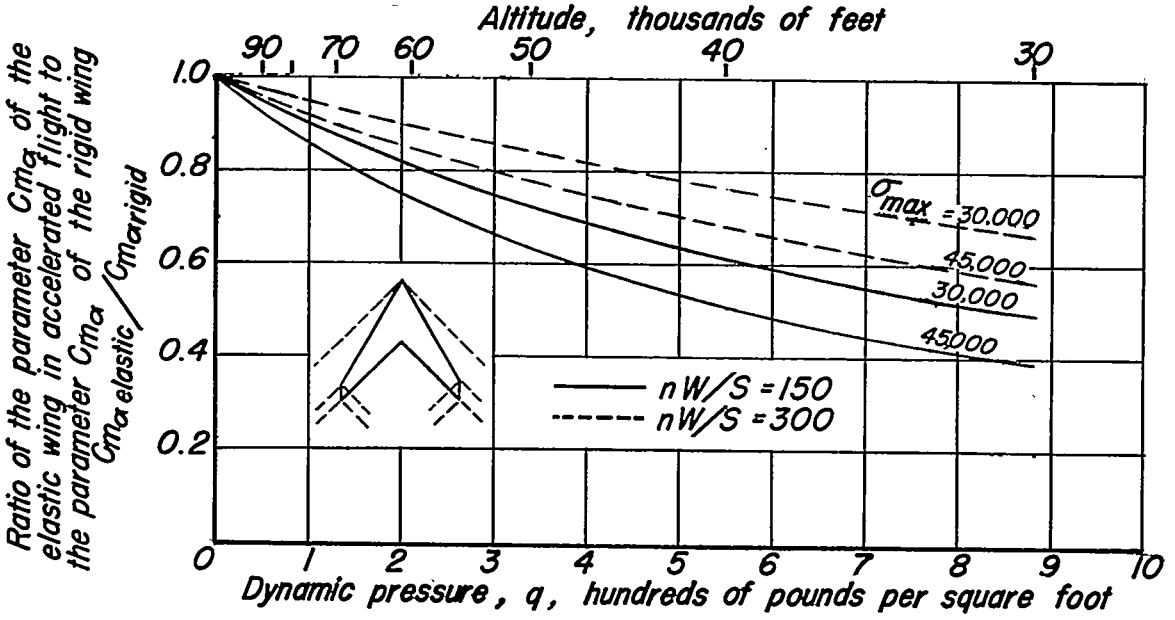

(a) Mach number, 1.414.

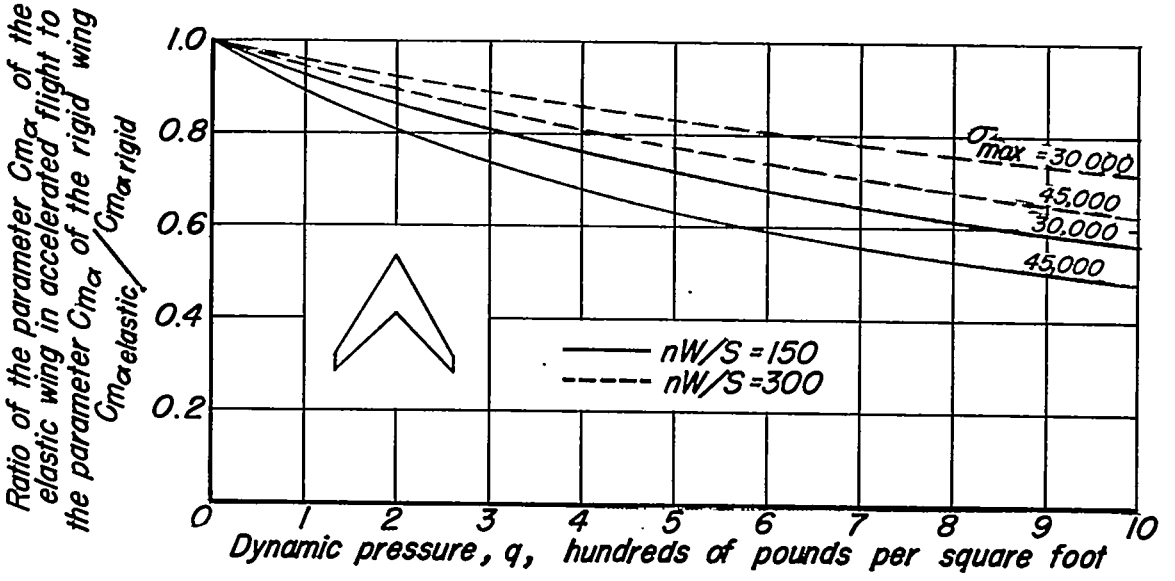

(b) Incompressible flow.

NACA

Figure 7. —Variation with dynamic pressure of the ratio of the parameters C_{m_α} for the elastic and rigid wings in accelerated flight.

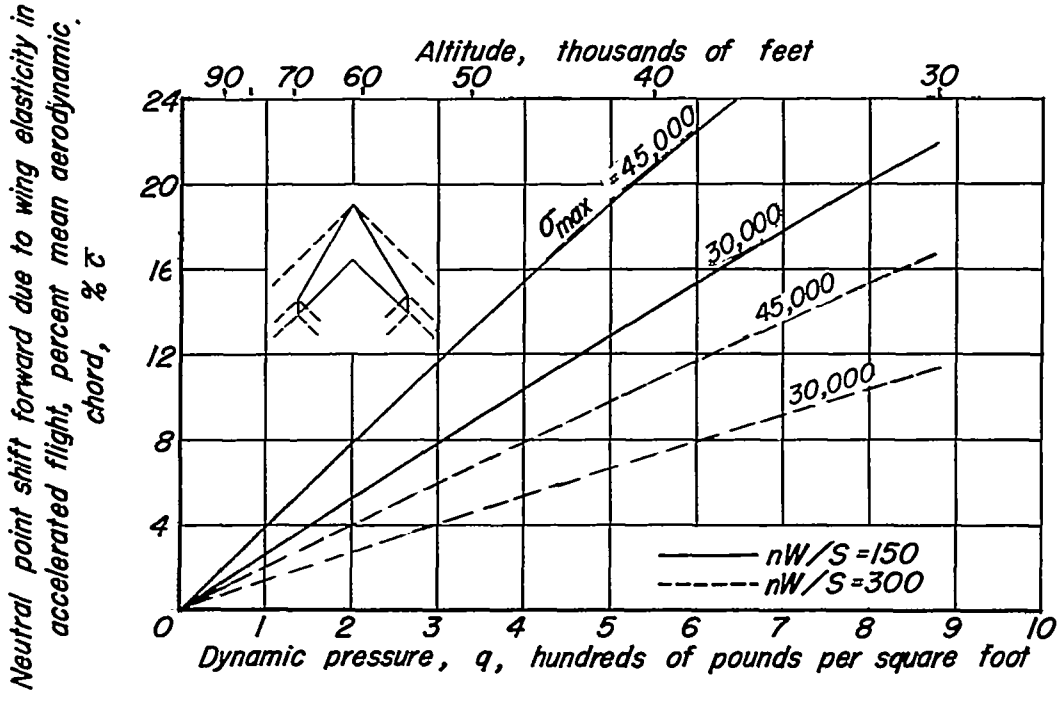

(a) Mach number, 1.414 .

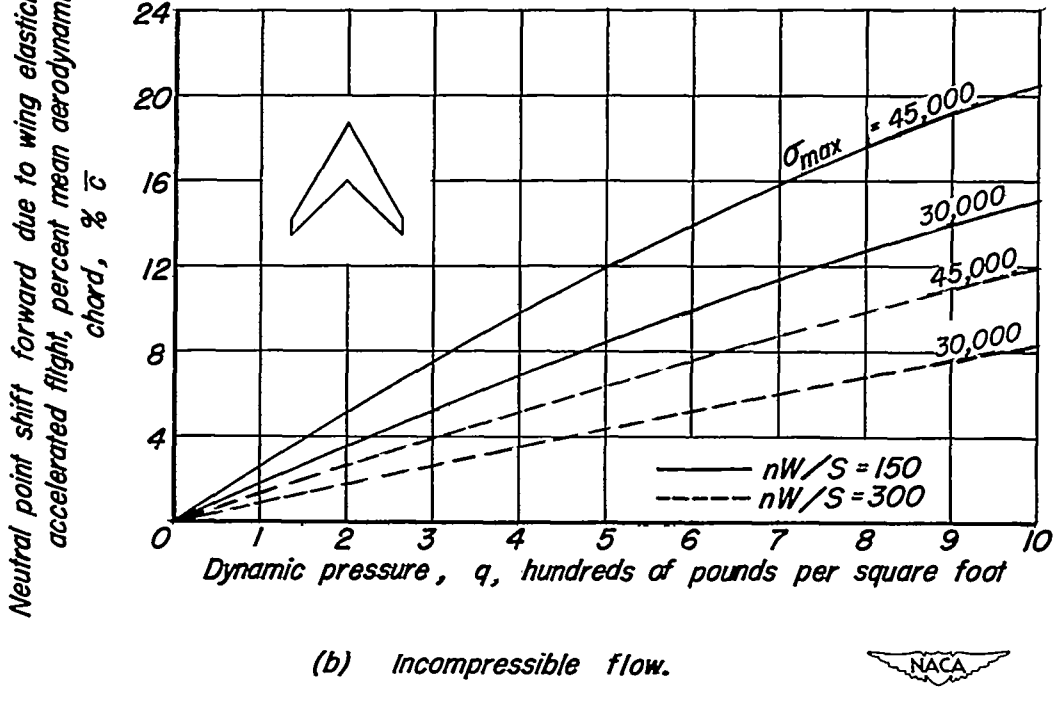

(b) Incompressible flow.

NACA

Figure 8. — Variation with dynamic pressure of the neutral point shift for the elastic wing in accelerated flight.